

# Using a geo-mechanical damage model to assess permeability in cracked porous media: internal length parameter issues

ARSON Chloé<sup>1</sup>

<sup>1</sup>Texas A&M University, Civil Engineering Department

carson@civil.tamu.edu

CE/TTI building, room 808-R, 3136 TAMU, College Station, TX 77843-3136, Texas, USA

Tel: 979-862-5659 Fax: 979-845-6554

**Keywords:** unsaturated porous media, damage model, permeability, internal length, REV, FEM

**Abstract.** The THHMD model is a thermo-hydro-mechanical damage model dedicated to unsaturated rocks. This work questions one of the postulates of its formulation, consisting in using the same Representative Elementary Volume (REV) to define the crack density tensor and to compute the damaged permeability. First, a drained triaxial compression test is simulated, by considering that the REV's dimension (noted  $b$ ) is a flow internal length. It shows that  $b$  can be used to scale the influence of damage on permeability. Secondly, a nuclear waste repository is modeled. Multiphase flow is studied in fractured porous bedrock subjected to heating. It is demonstrated that: 1. the THHMD model is mesh-independent, 2.  $b$  can be considered as the homogenization scale necessary to define the damage field, 3. the model can be improved by adding one internal length parameter in the formulation.

## Introduction

Multiphysics damage models are required to study important geotechnical problems, like the evolution of the Excavation Damage Zone in nuclear waste disposals (e.g. Blümling et al., 2007).

Models based on Continuum Damage Mechanics are often formulated by means of Bishop's effective stress. Damage is assumed to be barely mechanical and is not coupled to the poro-elastic behavior of the matrix. By contrast, fractures network models are focused on flow problems, and discard mechanical couplings. Combining both approaches is challenging. The THHMD model is a thermo-hydro-mechanical damage model dedicated to unsaturated rocks (Arson and Gatmiri, 2010). This paper questions the concept of Representative Elementary Volume (REV) used to model water permeability in a cracked porous medium. The first section explores different definitions for the REV, and explains the notion of effective properties. The theoretical frame of the THHMD model is briefly presented in the second section. The role of the internal length parameter introduced in the THHMD model is examined through numerical studies. The third section deals with a drained triaxial compression test performed on brittle sandstone. In the fourth section, a model of nuclear waste disposal is presented to study multiphase flow in a fractured porous rock.

## **Effective Continuum and Representative Element**

In *fracture flow models*, the pores of the intact (undamaged) matrix and the connected micro-cracks are considered as two networks, which may have different retention and permeability properties. In multimodal models (Durner, 1994), all kinds of voids are assumed to connect and to form a unique porous network (with a homogeneous pore pressure). In multi-continua models (e.g. Vogel et al., 2000), the natural porous network and the cracks network are assumed to drive fluid flows separately (with different pressure heads), but not always independently (fluid exchanges may occur between the matrix and the cracks). In all fractures network models, one of the challenges consists in determining the *equivalent flow properties* of a material element from the parameters of each network. The REV size is an important assumption of the model, because

permeability is scale-dependent (Guéguen et al., 1996). If the cracks are distributed on a periodic grid, the REV can be defined as the smallest geometric pattern necessary to reproduce the grid by juxtaposition. Pruess et al. (1990) thus defined an effective medium to model retention and permeability properties in fractured unsaturated tuff. Effective porosities ( $\bar{\phi}$ ) are computed as:

$$\bar{\phi}_m = \phi_m \frac{V_m}{V}, \quad \bar{\phi}_f = \phi_f \frac{V_f}{V} \dots\dots\dots(1)$$

in which  $V$  is the volume of the effective continuum (REV).  $\phi_m$  and  $\phi_f$  are the matrix and fractures porosities, respectively.  $V_m$  (respectively  $V_f$ ) is the volume occupied by the undamaged matrix (respectively by the fractures) in the REV. The effective degree of saturation is the sum of the degrees of saturation of each medium (matrix or fractures), weighted by the matrix and fractures effective porosities, respectively:

$$\bar{S}_w = \frac{\bar{\phi}_m S_{w,m} + \bar{\phi}_f S_{w,f}}{\bar{\phi}_m + \bar{\phi}_f} \dots\dots\dots(2)$$

The effective intrinsic permeability is the sum of the intrinsic permeabilities of both media ( $\bar{k}_m + \bar{k}_f$ ). The effective permeability relative to phase  $\beta$  ( $k_\beta$ ) is the sum of the relative permeabilities of both media, weighted by the corresponding intrinsic permeabilities:

$$k_\beta = \frac{\bar{k}_m k_{\beta,m} + \bar{k}_f k_{\beta,f}}{\bar{k}_m + \bar{k}_f} \dots\dots\dots(3)$$

*In Continuum Damage Mechanics*, the Representative Elementary Volume (REV) gives the scale at which an *effective stress* ( $\sigma_{ij}^{eff}$ ) can be defined to represent the stress effectively supported by the undamaged material surfaces. Using Cordebois and Sidoroff's operator (1982):

$$\sigma_{ij}^{eff} = M_{ijkl}(\Omega)\sigma_{lk} = (\delta - \Omega)_{il}^{-1/2} \sigma_{lk} (\delta - \Omega)_{kj}^{-1/2} \dots\dots\dots(4).$$

$\delta_{ij}$  is the second-order identity tensor and  $\Omega_{ij}$  is a second-order damage variable. The operator  $M_{ijkl}(\Omega)$ , relating effective and real stresses, quantifies the extent of the mechanical influence zone of the cracks. The damage variable used to model the mechanical effects of cracks depends on this influence zone, and is thus non-local (Bazant, 1991).

Homogenization methods can be used to upscale micro-mechanical state variables. Most of the homogenization techniques (e.g. dilute scheme, Mori-Tanaka scheme) fail at representing crack interactions at the scale of the REV. Recently, Zhu et al. (2008) proposed an integration scheme accounting for both the aspect ratio and the spatial distribution of the defects. The latter is defined by means of a density parameter. The cracks radius plays the role of an internal length parameter, which dictates the order of magnitude of the REV size. In hydro-mechanical models, flow regimes are determined by percolation thresholds. Even when cracks are not connected to each other, cracks can be connected to natural pores, which potentially increases permeability. As a result, at least one additional internal length parameter is required to set the upper bound of permeability in a cracked porous medium. Zhou et al. (2007) introduced the critical micro-crack length (when coalescence occurs). Other material parameters introduced by the authors are equivalent to internal lengths (e.g. hydraulic radius, pores geometric parameters).

### Theoretical Framework of the THHMD Model

The model examined in this paper (named THHMD model) is based Continuum Damage Mechanics, and is dedicated to non-isothermal unsaturated porous media (Arson and Gatmiri, 2010). The materials under study are constituted of a solid skeleton and of a porous network made of natural pores and cracks. The porous network is filled with liquid water (pore pressure

$p_l$ ) and with a gaseous mixture of dry air and vapor (pore pressure  $p_g$ ). It is assumed that cracks do not interact. Therefore, the loss of elastic deformation energy induced by cracking is only a function of the undamaged stiffness tensor and of the second-order crack density tensor (Kachanov, 1992). The damage variable is defined as a spectral decomposition of the second-order crack density tensor. Multi-directional cracking is thus represented by three equivalent cracks. The  $K^{\text{th}}$  equivalent crack is characterized by its volumetric fraction  $d^{(K)}$  and by the vector  $\mathbf{n}^{(K)}$ , normal to the  $K^{\text{th}}$  equivalent crack plane. Moreover, it is assumed that the equivalent cracks are penny-shaped, and that their apertures ( $e^{(K)}$ ) are related to their radius ( $r^{(K)}$ ) by a linear dilatancy rule. The damage variable thus writes:

$$\Omega_{ij} = \sum_{K=1}^3 d^{(K)} n_i^{(K)} n_j^{(K)} = \sum_{K=1}^3 \pi \chi \frac{(r^{(K)})^3}{b^3} n_i^{(K)} n_j^{(K)}, \quad \text{with} \quad \Delta e^{(K)} = \chi \Delta r^{(K)} \dots \dots \dots (5).$$

$\chi$  is the dilatancy parameter, and  $b$  is the characteristic dimension of the REV.

In the Excavation Damaged Zone (EDZ), families of non-connected cracks observed at the scale of the gallery are also observed at the scale of the laboratory samples (Blümling et al., 2007). It is thus justified to define a Representative Elementary Volume (REV), at the scale of which material parameters are homogenized under the assumption of cracks non-interaction. It is possible to model cracks at any scale, by resorting to the concept of equivalent crack density (Eq.5). If the homogenization scale of the REV is much larger than the typical crack length, the damage variable quantifies the porosity induced by three families of micro-cracks, characterized by their approximate parallel orientation. Three main crack-plane orientations define the eigenvectors of the damage tensor. If the homogenization scale of the REV is much smaller than the typical crack length, damage measures the fracture porosity in the plane of one crack.

The THHMD model is formulated in independent strain state variables: mechanical strain tensor  $\varepsilon_{M_{ij}}$ , volumetric capillary strains  $\varepsilon_{Sv}$  and volumetric thermal strains  $\varepsilon_{Tv}$ .  $\varepsilon_{M_{ij}}$ ,  $\varepsilon_{Sv}$  and  $\varepsilon_{Tv}$  are respectively conjugate to net stress ( $\sigma''_{ij} = \sigma_{ij} - p_g \delta_{ij}$ ), suction ( $s = p_g - p_l$ ) and thermal stress ( $p_T$ ). The state variables being independent, the increment of the total strain tensor is split as:

$$d\varepsilon_{ij} = \left( d\varepsilon_{M_{ij}}^e + d\varepsilon_{M_{ij}}^d \right) + \frac{1}{3} \delta_{ij} \left( \varepsilon_{Sv}^e + \varepsilon_{Sv}^d \right) + \frac{1}{3} \delta_{ij} \left( \varepsilon_{Tv}^e + \varepsilon_{Tv}^d \right) \dots \dots \dots (6)$$

in which e and d subscripts refer to elastic and inelastic deformations, respectively. The state laws are derived from the expression of Helmholtz free energy, which is assumed to be the sum of damaged elastic energies and crack closure potentials:

$$\begin{aligned} \Psi_s(\varepsilon_{M_{pq}}, \varepsilon_{Sv}, \varepsilon_{Tv}, \Omega_{pq}) = & \frac{1}{2} \varepsilon_{M_{ji}} D_{ijkl}(\Omega_{pq}) \varepsilon_{M_{ik}} + \frac{1}{2} \varepsilon_{Sv} \beta_s(\Omega_{pq}) \varepsilon_{Sv} + \frac{1}{2} \varepsilon_{Tv} \beta_T(\Omega_{pq}) \varepsilon_{Tv} \\ & - g_M \Omega_{ij} \varepsilon_{M_{ji}} - \frac{g_S}{3} \Omega_{ij} \delta_{ji} \varepsilon_{Sv} - \frac{g_T}{3} \Omega_{ij} \delta_{ji} \varepsilon_{Tv} \dots \dots \dots (7) \end{aligned}$$

in which  $D_{ijkl}(\Omega_{pq})$  is the damaged mechanical stiffness tensor,  $\beta_s(\Omega_{pq})$  is the damaged capillary modulus, and  $\beta_T(\Omega_{pq})$  is the damaged thermal modulus.  $D_{ijkl}(\Omega_{pq})$ ,  $\beta_s(\Omega_{pq})$  and  $\beta_T(\Omega_{pq})$  are determined by applying the Principle of Equivalent Elastic Energy.  $g_M$ ,  $g_S$  and  $g_T$  are the material resistance to mechanical, capillary and thermal cracking, respectively. The damage evolution law is inspired from the works of Dragon et al. (2000):

$$d\Omega_{ij} = d\lambda_d \frac{\partial f_d(Y_{d1_{pq}}^+, \Omega_{pq})}{\partial Y_{d1_{ij}}^+} \dots \dots \dots (8)$$

in which:

$$f_d(Y_{d1_{pq}}^+, \Omega_{pq}) = \sqrt{\frac{1}{2} Y_{d1_{ij}}^+ Y_{d1_{ji}}^+ - C_0 - C_1 \Omega_{ij} \delta_{ji}} \dots \dots \dots (9)$$

and:

$$Y_{d1_{ij}}^+ = g_M \epsilon_{M_{ij}}^+ + \frac{g_S}{3} \delta_{ij} \epsilon_{Sv}^- + \frac{g_T}{3} \delta_{ij} \epsilon_{Tv}^+ \dots \dots \dots (10).$$

$C_0$  is an initial energy release rate and  $C_1$  is a hardening parameter. The expression of  $Y_{d1_{ij}}^+$  is chosen to make damage grow with mechanical strains due to tensile stresses ( $\epsilon_{M_{ij}}^+$ ), pore shrinkage due to suction ( $\epsilon_{Sv}^-$ ) and dilatation due to temperature ( $\epsilon_{Tv}^+$ ).

The cracks non-interaction hypothesis does not imply that cracks do not constitute new flow paths. In geomaterials such as granite, salt rock or clay stone, cracks length is sufficiently large compared to the typical size of the natural matrix pores to assume that each crack is connected to the pores of the non-damaged skeleton (Maleki and Pouya, 2010). The cracks network is assumed to have its own intrinsic permeability ( $\bar{k}_f$ , Eq.3), which adds to the intrinsic permeability of the intact porous matrix ( $\bar{k}_m$ , Eq.3). This additional intrinsic permeability depends on the volume of the voids generated by cracking, and therefore, on the size and orientation of the equivalent cracks. It is thus a tensor ( $\bar{K}_{f_{ij}}$ ), depending on damage eigenvalues and eigenvectors. Assuming that the flow in the cracks is laminar makes it possible to model water transfer with the cubic law (Shao et al., 2005). For equivalent cracks (Eq.5), we have:

$$\bar{K}_{f_{ij}} = \frac{\gamma_w}{12\mu_w} \pi^{-2/3} \chi^{4/3} b^2 \sum_{K=1}^3 \left( d^{(K)} \right)^{5/3} \left( \delta_{ij} - n_i^{(K)} n_j^{(K)} \right) \dots \dots \dots (11).$$

$\gamma_w$  is water specific weight, and  $\mu_w$  is water dynamic viscosity.  $b$  is the REV's characteristic dimension, introduced in the definition of the homogenized damage variable (Eq.5).  $b$  also plays the role of an internal length parameter in the liquid flow problem.

### Scaling Permeability. Drained Triaxial Compression Test on a Brittle Rock.

This section aims at studying the influence of  $b$ , when used as a flow internal length parameter (Eq.11). A drained triaxial compression test performed on Fontainebleau sandstone is simulated with  $\Theta$ -Stock Finite Element code (Gatmiri and Arson, 2008). The results are compared to the experimental measurements reported in (Sulem and Ouffroukh, 2006). The Young's modulus, Poisson's ratio and mechanical damage parameters ( $g_M, C_0, C_1$ ) of sandstone are taken from (Dragon et al., 2000):  $E_0 = 4.55 * 10^{10} Pa$ ,  $\nu_0 = 0.3$ ,  $g_M = -1.1 * 10^8 Pa$  (Soil Mechanics sign convention: compressions counted positive),  $C_0 = 10^3 Pa$ ,  $C_1 = 5.5 * 10^5 Pa$ . According to Shao et al. (2005), the dilatancy parameter  $\chi$  is taken equal to 0.005. The initial void ratio of the undamaged sample ( $e_0$ ), and the intrinsic permeability of the damaged matrix in saturated conditions ( $k_{w0}$ ) are given in (Sulem and Ouffroukh, 2006):  $e_0 = 0.2658$ ,  $k_{w0} = 3.33 * 10^{-5} m/s$ . The material stays saturated during the whole test. The permeability to liquid water is (Eq.11):

$$K_{w_{ij}} = \bar{k}_m \delta_{ij} + \bar{K}_{f_{ij}} = k_{w0} \delta_{ij} + \frac{\gamma_w}{12\mu_w} \pi^{-2/3} \chi^{4/3} b^2 \sum_{K=1}^3 \left( d^{(K)} \right)^{5/3} \left( \delta_{ij} - n_i^{(K)} n_j^{(K)} \right) \dots \dots \dots (12)$$

In most of the existing modeling approaches, the REV size (or “scale of observation”)  $b$  cannot be determined directly. For instance, Shao et al. (2005) resort to a micro-mechanical framework, in which, for a given REV, it is necessary to assess the cracks sizes and number to evaluate the contribution of the cracks to hydraulic flow. On the other hand, several authors measured permeability in the field and in the lab. It is established (Zimmermann et al., 2003) that permeability of highly fractured zones is 100 to 1000 higher than in undamaged zones (where permeability is only a function of natural porosity). That is the reason why, in the THHMD



model, it is assumed that the damaged permeability is known for an isotropic damage of high intensity. Given a permeability measure  $\bar{K}_{fij} = k_{wdg}^{\max} \delta_{ij}$  for  $\Omega_{ij} = 0.95\delta_{ij}$ , we have (Eq.12):

$$b = \frac{\sqrt{6}}{0.95^{5/6}} \left( \frac{\pi}{\chi^2} \right)^{1/3} \left( \frac{\mu_w}{\gamma_w} \right)^{1/2} (k_{wdg}^{\max})^{1/2} \dots\dots\dots(13)$$

In the reference simulation presented in Fig.1 and Fig.2.a, the “maximal damaged permeability” is fixed to  $k_{wdg}^{\max} = 100k_{w0}$ , which corresponds to a permeability observation scale  $b$  of  $2.34 * 10^{-3} m$ . It has to be noted that the internal length parameter  $b$  does not play the same role as the hydraulic connectivity introduced by Shao et al. (2005) and by Zhou et al. (2007). In Eq.13,  $b$  is defined for a given permeability measured for a high density of non-connected cracks. On the contrary, the hydraulic internal length used in (Shao et al., 2005) and (Zhou et al., 2007) defines a percolation threshold reached when cracks coalesce.

The problem is axis-symmetric and isothermal. Fluid fluxes, shear stress and radial displacements are fixed to zero on the axis. Shear stress and vertical displacements are fixed to zero at the basis. During the confining phase, fluid fluxes are set to zero on all the outer boundaries, and a confining pressure of 28MPa is progressively applied at the top and lateral boundaries of the cell. During the compression phase, pore pressures are fixed to zero on all the outer boundaries, the confining pressure is maintained at the lateral boundary ( $\sigma_{rr}=28\text{MPa}$ ), and vertical stress ( $\sigma_{zz}$ ) is increased till the total failure of the sample.

The match between the experimental and numerical stress/strain curves is satisfactory (Fig.1.a). Damage predictions are in agreement with the model assumptions: the sample is in tension in both lateral directions, and in compression in the axial direction, so that crack planes develop in the directions normal to  $\mathbf{e}_r$  and  $\mathbf{e}_\theta$ . As a result, both lateral components of damage are

equal and non-zero, while vertical damage remains null:  $\Omega_{rr} = \Omega_{\theta\theta} \neq 0$ ,  $\Omega_{zz} = 0$  (Fig.1.b). Cracks perpendicular to  $\mathbf{e}_r$  contribute to water flow in  $\mathbf{e}_\theta$  and  $\mathbf{e}_z$  directions, and cracks perpendicular to  $\mathbf{e}_\theta$  contribute to water flow in  $\mathbf{e}_r$  and  $\mathbf{e}_z$  directions (Eq.11-12). Permeability thus increases in all directions, with  $K_{w_{zz}} > K_{w_{rr}} = K_{w_{\theta\theta}}$  (Fig.2.a).

Several orders of magnitude for the “maximal damaged permeability” are tested. For  $k_{wdg}^{\max} = k_{w0}$ ,  $k_{wdg}^{\max} = 10k_{w0}$ ,  $k_{wdg}^{\max} = 10^2 k_{w0}$ ,  $k_{wdg}^{\max} = 10^3 k_{w0}$  and  $k_{wdg}^{\max} = 10^4 k_{w0}$ , we respectively have:  $b = 2.34 * 10^{-4} m$ ,  $b = 7.39 * 10^{-4} m$ ,  $b = 2.34 * 10^{-3} m$ ,  $b = 7.39 * 10^{-3} m$  and  $2.34 * 10^{-2} m$ . The influence of  $k_{wdg}^{\max}$  (or  $b$ ) on permeability variations can be huge, as shown in Fig.2.b. If damage were 100% in all directions, the global permeability would increase by two orders of magnitude (Eq.11-12). In the reference case ( $k_{wdg}^{\max} = 10^2 k_{w0}$ ), the maximal value reached by the lateral damage component is less than 20% (Fig.1.b), which results in an increase of permeability of more than one order of magnitude (Fig.2.a). Similarly (Fig.2.b), permeability increases by: three orders of magnitude with  $k_{wdg}^{\max} / k_{w0} = 10^4$ , two with  $k_{wdg}^{\max} / k_{w0} = 10^3$ , and less than one for  $k_{wdg}^{\max} / k_{w0} = 10$  and  $k_{wdg}^{\max} / k_{w0} = 1$ . As a conclusion,  $b$  can be used as a flow internal length.

### Scaling Initial Crack Density. Heating an Unsaturated Cracked Porous Rock.

A nuclear waste repository excavated in fractured unsaturated tuff is modeled to study the influence of  $b$ , when used as a damage homogenization scale (the REV size required to define a crack density, Eq.5). Waste is disposed in vertical boreholes, as shown in Fig.3. In the initial state, horizontal cracks are present in the rock mass. The spacing is 0.22m. The cracks' aperture is  $\delta_f = 0.002m$  and the fractures' porosity is  $\phi_f = 0.2$ . It is assumed that damage remains constant (i.e.  $g_M = g_S = g_T = 0$ ). The configuration is axis-symmetric. The domain spreads from

$R=0.25\text{m}$  to  $R=10\text{m}$ . Waste is considered as a heating source of decreasing power, which sets a heat flux boundary condition at the inner radius of the domain. The initial power per waste package is  $3.051\text{ kW}$ , and the waste is assumed to be 10 years old. The radioactive package length is not provided in the reference article (Pruess et al., 1990). In this study, it is assumed that each package is 5 meters long and the corresponding surface powers are computed by using the relative powers indicated in (Pollock, 1986).

The problem is simulated with  $\Theta$ -Stock Finite Element program (Gatmiri and Arson, 2008). The fractured zones are modeled by elements with a non zero initial damage tensor (Eq.5). Provided that fractures are horizontal, only the vertical component of damage ( $\Omega_{zz}^0$ ) is non-zero. The results obtained with the THHMD model are compared to Pruess et al.'s predictions (1990). Interpretations are less straightforward than in the previous numerical example, because the two modeling approaches are different. In Pruess et al.'s model, the natural pores and the cracks are two distinct continua, which are assumed to be in thermodynamic equilibrium. Equivalent porosity, saturation degree and permeability are deduced from the properties of each network (Eq.1-3). By contrast, the THHMD model is similar to a bimodal model, in which damage growth results in a global porosity increase (in the ranges of pore sizes corresponding to the typical cracks length) and in a global permeability increase (Eq.5-11).

To follow the pure thermo-hydraulic approach of Pruess et al. (1990), all nodal displacements are neutralized. Initial temperature and pore pressures are maintained at the external radius of the domain. The main material parameters are provided in Pruess et al.'s paper:  $\phi_m = 0.103$ ,  $\bar{k}_m = 3.26 * 10^{-10} \text{ m/s}$ . The evolution of the degree of saturation is given by:

$S_w = \left[ 1 + \left( 7.179 * 10^{-7} * |p_g - p_l| \right)^{1.818} \right]^{-0.45}$ . The rock specific heat and thermal conductivity are

respectively:  $C_T = 769 \text{ J/(kg} \cdot ^\circ\text{C)}$  and  $\lambda_T = 1.6 \text{ W/(m} \cdot ^\circ\text{C)}$ . In the initial state, temperature equals  $26^\circ\text{C}$ . Pruess et al. assume that initial gas pore pressure is  $10^5 \text{ Pa}$  and that the initial matrix degree of saturation is 0.8. With  $\Theta$ -Stock, gas pore pressure is initialized by inverting the formula of the degree of saturation, with  $S_w^0 = 0.8$ . Two sets of simulations are performed:

1. *Influence of the damage homogenization scale.* Only one fracture is modeled, by setting a non-zero damage tensor on the central elements of the mesh. Mesh changes induce a crack density change, as described in Tab.1.
2. *Influence of mesh refinement.* Eight fractures are present in the domain. In this set of simulations, all elements of the domain are initially damaged. Moreover, the Finite Element sizes are chosen so that the initial crack density be the same on all the elements and in all simulations. Five mesh refinements are tested (Tab.2).

In the nuclear waste disposal modeled in this study, a horizontal crack crossing a Finite Element of characteristic dimension  $b$  is a penny-shaped cylinder with a normal vector  $\mathbf{e}_z$ , a radius  $b/2$  and a thickness  $\chi b/2$ . Therefore, the initial damage field is:

$$\Omega_{ij}^0 = \Omega_{zz}^0 e_{z_i} e_{z_j} = d^{0(z)} e_{z_i} e_{z_j} = \frac{\pi(b/2)^2 \chi(b/2)}{b^3} e_{z_i} e_{z_j} = \frac{\pi\chi}{8} e_{z_i} e_{z_j} \dots\dots\dots(14).$$

The aperture of the fractures is  $\delta_f$ , but the volume of void generated by cracking is weighted by the fractures' porosity  $\phi_f$ . The dilatancy parameter is thus defined as:

$$\chi = \frac{\delta_f}{(b/2)} \phi_f \dots\dots\dots(15).$$

For each of the nine meshes described above, the simulation has been run in an initially damaged rock mass (Tab.1-2) and in an intact (undamaged) formation. The degree of saturation

evolution is the same for all meshes. Despite some differences with the results reported in the reference article (Pruess et al., 1990), the evolution of the degree of saturation in space and time can be interpreted by the same physical phenomena. In intact tuff (Fig.4.a), the rock mass surrounding the canister dries. The degree of saturation is zero at the borehole wall ( $R=0.25\text{m}$ ). The zone of influence of the heating source continues extending up to  $R=6\text{m}$ , even after the peak temperature is reached (at  $t=5$  years). Close to the heating source, pore water vaporizes. Due to the increase of gas pressure near the canister, vapor is conveyed in the far field. In this colder region, vapor condensates, and is driven back to the source by capillary effects. That is the reason why the extent of the dried zone reduces after 10 years of storage. Even after 100 years of decreasing heating, the degree of saturation in the vicinity of waste remains almost zero. When initial damage is introduced (Fig.4.b), fractures are modeled as high-permeability regions. The movement of vapor condensate towards low-water pressure areas is not only conveyed by the matrix, but also by the cracks. Transfer of condensate is so fast that it partially compensates the drying process. At the vicinity of the heating source, the degree of saturation decreases to 0.4 (instead of 0 in intact tuff). After 5 years, when temperature starts to decrease, the dried zone starts to saturate again, due to the movement of condensate.

The temperature predictions are the same in the 18 simulations. Near the canister, the temperature peaks at around  $260^{\circ}\text{C}$  after five years of heating (Fig.5). An exponent decrease is observed in space (as the distance to the heating source is increased) and time (as the heating power gets lower). This is in conformity with the results obtained by Pruess et al. for intact tuff. In fractured rock, the damage model cannot predict the same evolutions as Pruess et al.'s model because the homogenized retention and permeability properties are not computed in the same way. In the damage model, retention properties are the same for damaged and intact elements, so

that liquid is not forced to go through the porous matrix by capillary effects. Despite this liquid mobility, the damage model predicts an inner conductive zone. This may be due to a difference in the way initial gas pore pressure is initialized.

## Conclusion

The concept of internal length parameter is investigated through numerical parametric studies performed with the THHMD model (thermo-hydro-mechanical damage model for unsaturated rocks). The damage variable is the spectral decomposition of the second-order crack density tensor. A single internal length parameter ( $b$ ) is introduced to ensure the validity of the continuum-based modeling approach on both the mechanical point of view (crack density and damaged stiffness) and the hydraulic point of view (flow paths and permeability variations associated to cracking).

A drained triaxial compression test performed on sandstone is simulated. A parametric study shows that  $b$  can be considered as an input parameter scaling the permeability variations in function of the rate of damage. The THHMD model is also used to study non-isothermal multiphase flow in a fractured porous medium. The presence of fractures in the bedrock is modeled by setting a non-zero initial damage field on some elements of the mesh. In a first set of simulations, one fracture is modeled with various homogenization scales. In a second set of simulations, the element sizes are fitted to have a homogeneous initial damage field in a domain containing eight fractures. The results are in conformity with the reference data found in the literature, and provide the same predictions for different mesh refinements. Therefore: 1. the parameter  $b$  can be considered as the homogenization scale required to define the damage field, 2. the THHMD model is mesh-independent.

In the THHMD model, the characteristic length used to define the crack density tensor ( $b$ ) is the same as the internal length required to compute the damaged permeability. If  $b$  is chosen to scale permeability, then  $b$  may not correspond to the Finite Element size required to initialize the damage field. On the contrary, if  $b$  is chosen to scale the initial crack density tensor, then  $b$  may not correspond to a realistic flow internal length parameter. A fracture network is characterized by cracks locations, lengths, apertures and orientations. The proposed damage model only accounts for crack density and crack orientation, which means that the cracks' locations, lengths and apertures are merged into one single variable. The THHMD model may be improved by adding an internal length parameter in the formulation.

## References

Arson, C. and Gatmiri, B., Numerical study of a thermo-hydro-mechanical model for unsaturated porous media, *Annals of Solid and Structural Mechanics*, vol. 1, n. 2, pp. 59-78, 2010.

Bazant, Z., Why continuum damage is non local: micromechanics arguments, *Journal of Engineering mechanics, ASCE*, vol. 117, n. 5, pp. 1070-1087, 1991.

Blümling, P., Bernier, F., Lebon, P. and Derek Martin, C., The excavation damaged zone in clay formations. Time-dependent behaviour and influence on performance assessment,, *Physics and Chemistry of the Earth*, vol. 32, pp. 588-599, 2007.

Cordebois, J.P. and Sidoroff, F., Endommagement anisotrope en élasticité et plasticité, *Journal de Mécanique théorique et appliquée*, special issue, pp. 45-60, 1982.

Dragon, A., Halm, D. and Désoyer, T., Anisotropic damage in quasi-brittle solids: modelling, computational issues and applications, *Comput. Methods Appl. Mech. Engrg.*, vol. 183, pp. 331–352, 2000.

- Durner, W., Hydraulic conductivity estimation for soils with heterogeneous pore structure, *Water Resour. Res.*, vol. 30, n. 2, pp. 211-223, 1994.
- Gatmiri, B. and Arson, C.,  $\Theta$ -Stock, a powerful tool for thermohydromechanical behaviour and damage modelling of unsaturated porous media, *Computers and Geotechnics*, vol. 35, n. 6, pp. 890-915, 2008.
- Guéguen, Y., Gravilenko, P. and Le Ravalec, M., Scales of Permeability, *Surveys in Geophysics*, vol. 17, pp. 245-263, 1996.
- Kachanov, M., Effective elastic properties of cracked solids: critical review of some basic concepts, *Appl. Mech. Rev.*, vol. 45, n. 8, pp. 304-335, 1992.
- Maleki, K. and Pouya, A., Numerical simulation of damage–Permeability relationship in brittle geomaterials, *Computers and Geotechnics*, vol. 37, pp. 619-628, 2010.
- Pollock, D.W., Simulation of Fluid Flow and Energy Transport Processes Associated With High-Level Radioactive Disposal in Unsaturated Alluvium, *Water Resources Research*, vol. 22, n. 5, pp. 765-775, 1986.
- Pruess, K., Wang, J.S.Y. and Tsang, Y.W., On Thermohydrologic Conditions Near High-Level Nuclear Wasters Emplaced in Partially Saturated Fractured Tuff. 2. Effective Continuum Approximation, *Water Resources Research*, vol. 26, n. 6, pp. 1249-1261, 1990.
- Shao, J.F., Zhou, H. and Chau, K.T., Coupling between anisotropic damage and permeability variation in brittle rocks, *International Journal for Numerical and Analytical Methods in Geomechanics*, vol. 29, pp. 1231–1247, 2005.



Sulem, J. and Ouffroukh, H., Shear banding in drained and undrained triaxial tests on a saturated sandstone: porosity and permeability evolution, *International Journal of Rock Mechanics and Mining Sciences*, vol. 43, pp. 292–310, 2006.

Vogel T., Gerke, H.H., Zhang, R. and Van Genuchten, M.T., Modeling flow and transport in a two-dimensional dual-permeability system with spatially variable hydraulic properties, *J. Hydrol.*, vol. 238, pp. 78-89, 2000.

Zhou, H., Shao, J.F., Feng, X.T. and Hu, D.W., Coupling Analysis between Stress Induced Anisotropic Damage and Permeability Variation in Brittle Rocks, *Key Engineering Materials*, vol. 340-341, pp. 1133-1138, 2007.

Zhu, Q.Z., Kondo, D. and Shao, J.F., Micromechanical analysis of coupling between anisotropic damage and friction in quasi brittle materials: Role of the homogenization scheme, *International Journal of Solids and Structures*, vol. 45, pp. 1385-1405, 2008.

Zimmermann, G., Burkhardt, H. and Engelhard, L., Scale Dependence of Hydraulic and Structural Parameters in the Crystalline Rock of the KTB, *Pure Appl. Geophys.*, vol. 160, pp. 1067-1085, 2003.

## TABLES

**Table 1. Element Sizes for the Set of Simulations 1: Damaged and Undamaged Elements.  
1 central crack of aperture 0.002m. Mesh extent: H=0.22m, L=10m.**

Number of elements per vertical section	Thickness of the damaged elements [m]	$d_z^0$	$\chi$	Position of the top intact elements [m]
8	0.001	0.1570	0.4000	0.001<z<0.005
				0.005<z<0.020
				0.020<z<0.110
6	0.005	0.0300	0.0800	0.005<z<0.020
				0.020<z<0.110
4	0.020	0.0079	0.02000	0.020<z<0.110
2	0.110	0.0010	0.00364	none

**Table 2. Element Sizes for the Set of Simulations 2: Damaged Elements Only.**

**1 crack of aperture 0.002m every 0.22m. Mesh extent: H=1.76m, L=10m.**

<b>Number of elements per vertical section</b>	<b>Number of cracks per element</b>	<b>Thickness of the elements [m]</b>	<b><math>d_z^0</math></b>	<b><math>\chi</math></b>
16	0.5	0.11	0.0010	0.00364
8	1	0.22		
4	2	0.44		
2	4	0.88		
1	8	1.76		

## FIGURES

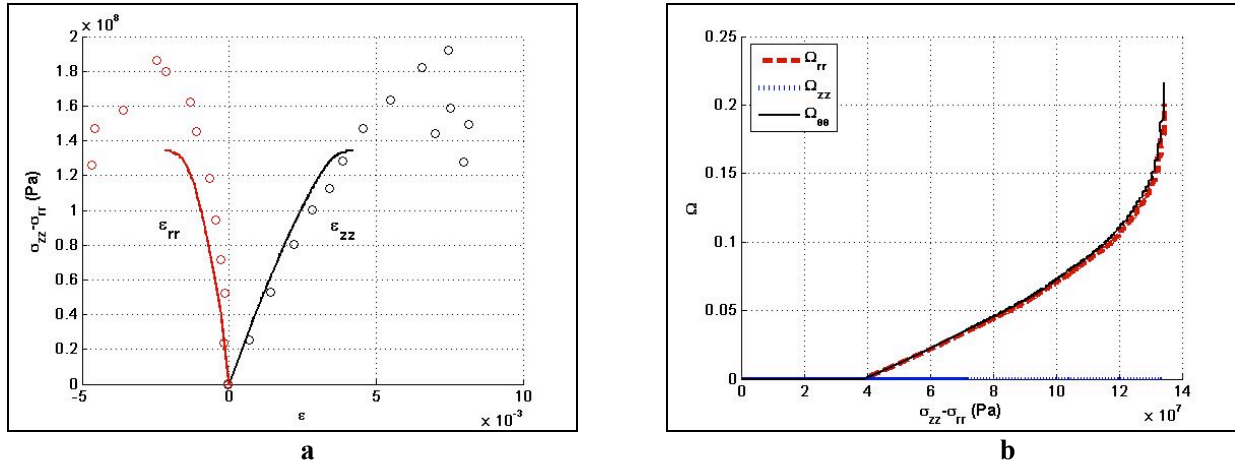


**Figure 1. Simulation of a Drained Triaxial Compression Test Performed on Fontainebleau Sandstone, with a Confining Pressure of 28MPa. a. Stress/strain Curve (plotted with the Soil Mechanics Sign Convention). Dots: Experimental Data from (Sulem and Ouffroukh, 2006). Solid Lines: Results Obtained with  $\Theta$ -Stock. b. Evolution of the Components of the Damage Tensor with Deviatoric Stress.**

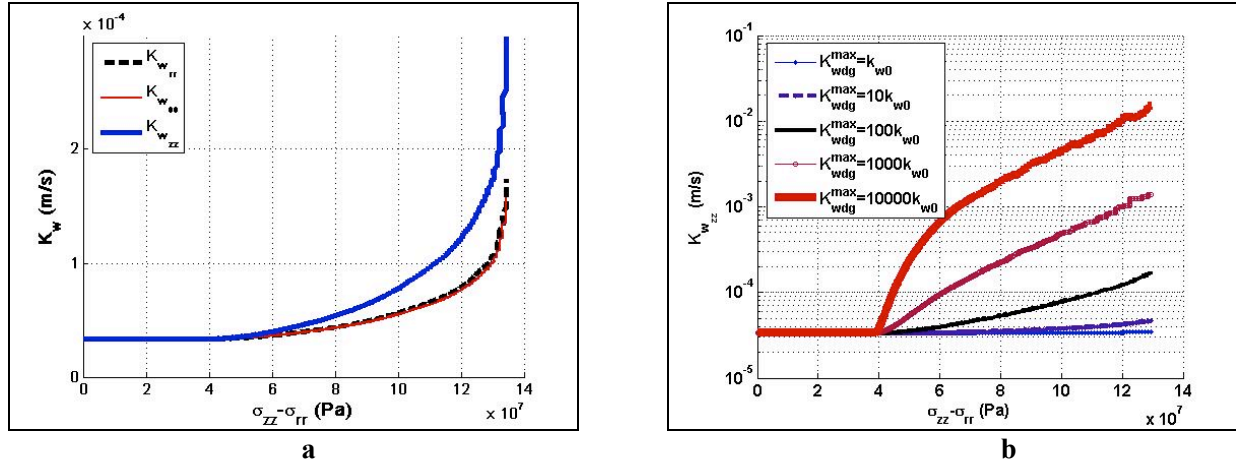


**Figure 2. Permeability Evolution in the Drained Triaxial Compression Tests Performed on Sandstone. a. Reference Simulation,  $k_{wdg}^{max} = 100k_{w0}$ . b. Parametric Study on  $b$  computed from  $k_{wdg}^{max}$  (Eq.13).**

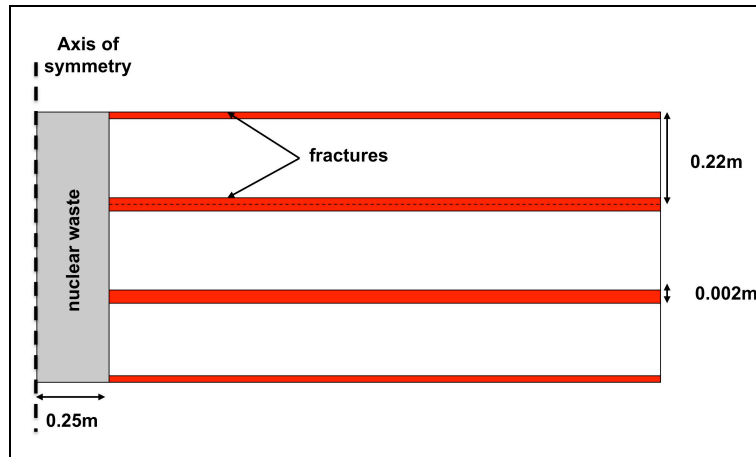


**Figure 3. Heating Test in Unsaturated Fractured Tuff: Geometry of the Problem.**

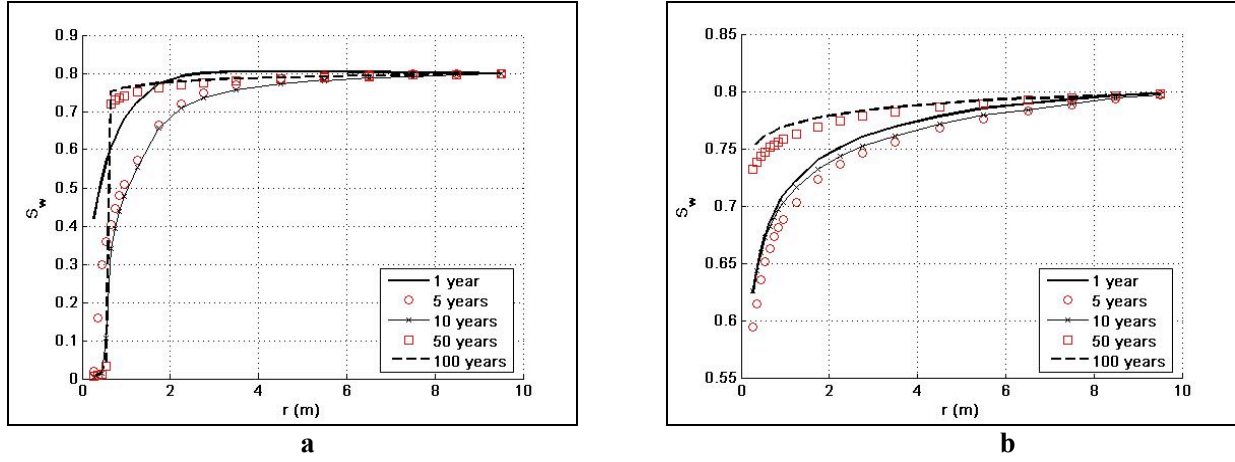


**Figure 4. Evolution of the Degree of Saturation (Same predictions for All Meshes).**  
**a. Intact Tuff (Zero Damage). b. Fractured Tuff (Non Zero Initial Damage Tensor, Tab.1-2).**

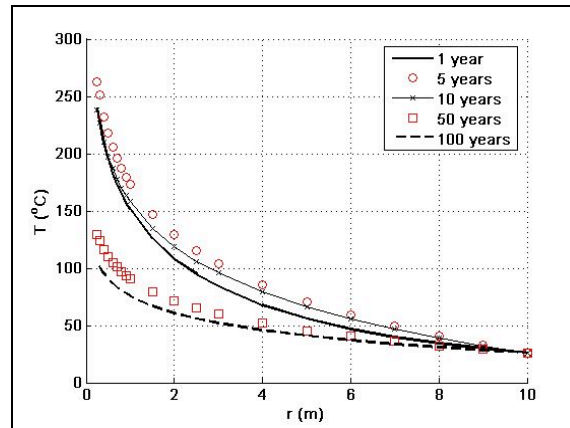


**Figure 5. Temperature Distribution (Same in Intact and Fractured Tuff, and Same for All Meshes).**